Fundamental electron-transfer and proton-coupled electron-transfer properties of Ru(iv)-oxo complexes

doi: 10.1039/C9DT02734C

ARTICLE

Fundamental electron-transfer and proton-coupled electron-transfer properties of Ru(IV)-oxo complexes

Received 00th January 20xx,
Accepted 00th January 20xx

DOI: 10.1039/x0xx00000x

Hiroaki Kotani,[a] Hinatsu Shimomura,[a] Momoka Horimoto,[a] Tomoya Ishizuka,[a] Yoshihito Shiota,[b] Kazunari Yoshizawa,[b] Sachiko Yanagisawa,[c] Yuka Kawahara-Nakagawa,[c] Minoru Kubo[c] and Takahiko Kojima*[a]

Isolation and characterization of $Ru^{IV}(O)$ complexes were accomplished to investigate their fundamental electron transfer (ET) and proton-coupled ET (PCET) properties. Reorganization energies (λ) in electron transfer (ET) and proton-coupled ET (PCET) from electron donors to the isolated $Ru^{IV}(O)$ complexes have been determined for the first time to be in the range of 1.70–1.88 eV (ET) and 1.20–1.26 eV (PCET). It was suggested that the reduction of the λ values of PCET in comparison with those of ET should be due to the smaller structural chage in PCET than that in ET on the basis of DFT calculations on **1** and $1e^-$-reduced **1** in the absence and presence of TFA, respectively. In addition, the smaller λ values for the $Ru^{IV}(O)$ complexes than those reported for $Fe^{IV}(O)$ and $Mn^{IV}(O)$ complexes should be due to the lack of participation of d_σ orbitals in the ET and PCET reactions. This is the first example to evaluate fundamental ET and PCET properties of $Ru^{IV}(O)$ complexes leading to further understanding of their reactivity in oxidation reactions.

Introduction

High-valent metal-oxo complexes ($M^{n+}(O)$) have been recognized to play crucial roles in oxidation reactions as a key intermediate.[1] So far, extensive efforts have been devoted to a development of $M^{n+}(O)$ to elucidate their reactivity in oxidation reactions.[2,3] These oxidative reactions have been triggered by hydrogen-atom transfer from C-H bonds of organic substrates to $M^{n+}(O)$. In the course of the reactions, $M^{n+}(O)$ can accept a proton and an electron as a net hydrogen-atom transfer ($H\bullet = H^+ + e^-$) *via* a proton-coupled electron transfer (PCET) mechanism.[4] As shown in Scheme 1, PCET includes concerted proton-electron transfer (CPET), in which one H^+ and one e^- are transferred in a single kinetic step, and stepwise pathways involving electron transfer (ET) followed by proton transfer (PT) and PT followed by ET, which are mentioned as ET/PT and PT/ET, respectively. In addition, at the beginning of CPET reactions by $M^{n+}(O)$, the interaction of proton with the oxo ligand should facilitate ET from electron donors to $M^{n+}(O)$ to induce positive shifts of the redox potentials.[4] Therefore, the reactivity of $M^{n+}(O)$ in oxidation reactions is related to their controlling factors in PCET.

Recently, fundamental ET and PCET properties of $M^{n+}(O)$ such as a reorganization energy (λ), which is determined on the basis of the Marcus theory of ET, have been recognized as one of factors to elucidate the reactivity of the $M^{n+}(O)$ species.[5,6] For instance, Mayer and co-workers have suggested that the rate constants in hydrogen-atom transfer reactions by $M^{n+}(O)$ could be estimated on the basis of the Marcus cross relation.[3a,7] So far, the λ values of ET and PCET reactions for an Fe^{IV}-oxo complex, $[Fe^{IV}(O)(N4Py)]^{2+}$, have been reported to be the same (λ = 2.74 eV).[6a,b] The generality of the conclusion, however, has yet to be assured; because the PCET reactivity depends on the proton acceptability of the basic ligand that is the oxo ligand for $M^{n+}(O)$ and the electron-acceptability of the metal centre,[8] both of which depend on the metal centres. Thus, investigation on ET and PCET properties of $M^{n+}(O)$ is still required not only for $M^{n+}(O)$ of the first-row transition metals but for that of the second-row transition metals. As a target of the scrutiny on ET and PCET properties of the second-row $M^{n+}(O)$, we have chosen $Ru^{IV}(O)$ species. High-valent Ru-oxo complexes have also been intensively investigated as active species in substrate oxidation reactions.[7a,9-12] However, the determination of λ values of either ET or PCET reactions has yet to be reported for high-valent Ru-oxo complexes.

We report herein the first determination of the λ values of ET and PCET for an isolated Ru^{IV}-oxo complex, $[Ru^{IV}(O)(MeBPA)(bpy)]^{2+}$ (**1**; MeBPA = *N*-methyl-*N*,*N*-bis(2-pyridylmethyl)amine), bpy = 2,2'-bipyridyl) and a well-known $Ru^{IV}(O)$ complex, $[Ru^{IV}(O)(bpy)_2(py)]^{2+}$ (**2**; py = pyridine)[7a,10a] as shown in Fig. 1.

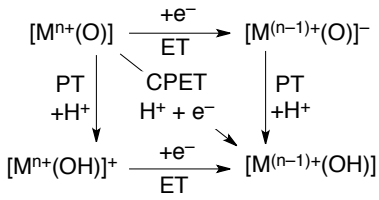

Scheme 1 PCET mechanism by metal-oxo complexes

[a] *Department of Chemistry, Graduate School of Pure and Applied Sciences, University of Tsukuba and CREST (JST), 1-1-1 Tennoudai, Tsukuba, Ibaraki 305-8571 (Japan) E-mail: kojima@chem.tsukuba.ac.jp.*
[b] *Institute for Materials Chemistry and Engineering, Kyushu University, Motooka, Nishi-Ku, Fukuoka 819-0395 (Japan).*
[c] *Graduate School of Life Science, University of Hyogo, 3-2-1 Koto, Kamigori-cho, Ako-gun, Hyogo 678-1297 (Japan).*

†Electronic Supplementary Information (ESI) available: [details of any supplementary information available should be included here]. See DOI: 10.1039/x0xx00000x

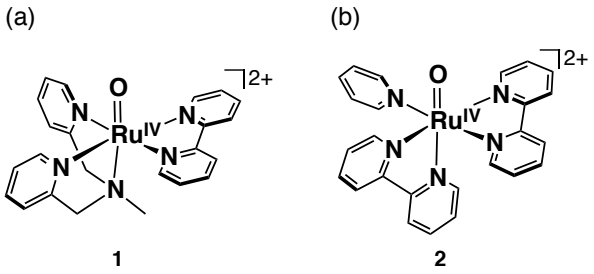

1 2

Fig. 1 Chemical structures of (a) $[Ru^{IV}(O)(Mebpa)(bpy)]^{2+}$ (**1**) and (b) $[Ru^{IV}(O)(bpy)_2(py)]^{2+}$ (**2**).

Results and discussion

Synthetic procedures

A precursor Ru(II)-aqua complex, $[Ru^{II}(Mebpa)(bpy)(OH_2)]^{2+}$ (**3**), was prepared by following the reported procedure[13] and its crystal structure was determined by X-ray crystallography (Fig. S1 in the ESI†). As compared to the reported structure of $[Ru^{II}(bpea)(bpy)(OH_2)]^{2+}$ (bpea = *N,N*-bis(2-pyridylmethyl)-ethylamine),[13] no structural change was observed by introducing a methyl group on the N atom instead of an ethyl group. Then, synthesis of **1** was accomplished by addition of $(NH_4)_2[Ce^{IV}(NO_3)_6]$ (CAN) as an oxidant to **3** in water as described in the experimental section. Similarly, complex **2** was synthesized by the reported procedure.[10b] Crystal structures of **1** and **2** were successfully determined by X-ray crystallography (Fig. 2). Although complex **2** has been known for a long time, this is the first report on the crystal structure. In the case of **1**, the oxo ligand located at the trans position of the tertiary amino group of the Mebpa moiety as expected from the structure of **3**. The oxo ligand of **2** bound at the trans position of one of pyridyl moieties of the bpy ligands. The Ru-O bond lengths (1.769(5) Å for **1**, 1.794(7) Å for **2**) are within the range of the previously reported values of $Ru^{IV}(O)$ (1.718–1.862 Å).[12c] As a strong evidence to support the formation of **1**, resonance Raman spectroscopy allowed us to observe a Raman scattering due to the $Ru^{IV}(^{16}O)$ vibration ($\nu_{Ru\text{-}O}$) at 797 cm^{-1}, which shifted to 760 cm^{-1} ($\Delta\nu$ = 37 cm^{-1}) in the case of ^{18}O-labeled $Ru^{IV}(^{18}O)$ as shown in Fig. S2 in the ESI†.[10c] The observed isotropic shift was consistent with the calculated value ($\Delta\nu$ = 38 cm^{-1}).

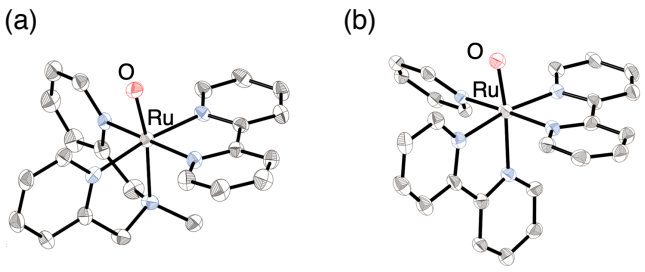

Fig. 2 ORTEP drawings of a) $[Ru^{IV}(O)(Mebpa)(bpy)]^{2+}$ (**1**) and b) $[Ru^{IV}(O)(bpy)_2(py)]^{2+}$ (**2**). Hydrogen atoms and counter ions were omitted for clarity. (c) An ORTEP drawing of **2** with 50% probability thermal ellipsoids. Hydrogen atoms and counter ions were omitted for clarity.

Redox Properties of $Ru^{IV}(O)$ complex

The one-electron reduction potentials (E_{red}) of **1** and **2** in acetonitrile (CH_3CN) at 298 K were determined to be 0.01 V *vs.* SCE and 0.17 V, respectively, by cyclic voltammetry (CV) and square wave voltammetry (SWV) as shown in Fig. S3 in the ESI†. The reversible redox couples indicate a formation of reduced species of $Ru^{IV}(O)$ complexes such as Ru^{III} complexes[14] are both stable under the experimental conditions.

Next, chemical reduction of **1** was performed by addition of decamethylferrocene ($Me_{10}Fc$; E_{ox} = –0.08 V *vs.* SCE)[15] to **1** in CH_3CN. The ET reaction was confirmed to be a $1e^-$ process by UV-vis spectral titrations of $Me_{10}Fc$, where the absorption band at 490 nm due to Ru^{III} species increases accompanied by an increase of the absorption band at 780 nm due to the corresponding ferricenium ion ($Me_{10}Fc^+$) as shown in Fig. S4 in the ESI†. In addition, the formation of the Ru^{III} species was also confirmed by electron spin resonance (ESR) spectroscopy (Fig. S5 in the ESI†). The observed ESR signal at g = 1.91, 2.16, and 2.32 is characteristic for Ru(III) species with the rhombic anisotropy.[12b,16] When octamethylferrocene (Me_8Fc; E_{ox} = –0.04 V *vs.* SCE)[17] was employed as an electron donor, the concentration of Ru^{III} species increased with saturation behavior rather than a stoichiometric reaction (Fig. S6a in the ESI†), indicating that the ET reaction reached to an ET equilibrium.[18] The ET equilibrium between $Ru^{IV}(O)$ and Me_8Fc was analyzed on the basis of the Nernst equation (eqn 1),

$$E_{red}' = E_{ox} + (RT/F)\ln K_{et} \quad (1)$$

where F is the Faraday constant and K_{et} is an ET-equilibrium constant.[17] The K_{et} value was determined to be 13 ± 8 at 243 K by fitting the plot as shown in Fig. S6a in the ESI†. Based on eqn 1, the apparent one-electron reduction potential (E_{red}') of **1** was determined to be 0.01 ± 0.01 V, which was consistent with that obtained by the aforementioned CV measurement. In addition, the E_{red}' value of **2** (0.14 V) was also determined by the same method with use of 1,2,3,4,5-pentamethylferrocene (Me_5Fc; E_{ox} = 0.15 V *vs.* SCE)[19] as an electron donor (Fig. S6b in the ESI†). The ET equilibrium between $Ru^{IV}(O)$ complexes and ferrocenes indicates the formation of Ru^{III} species including the naked oxo moiety as a $Ru^{III}(O)$ complex without protonation of the oxo ligand, as confirmed by DFT calculations including two H_2O molecules interacting with the oxo ligand *via* hydrogen bonding (Fig. 3).

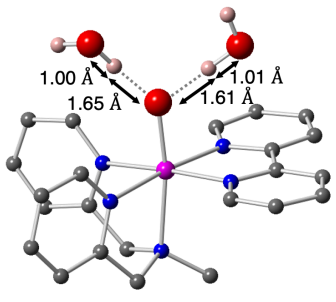

Fig. 3 A DFT optimized structure of $Ru^{III}(O)$ with two hydrogen-bonded H_2O molecules.

ET and PCET reactions by $Ru^{IV}(O)$ complex

In order to determine the ET rate constants (k_{et}) from electron donors to **1** and **2** in CH_3CN, we employed a series of ferrocenes ($Me_{10}Fc$, Me_8Fc, and Me_5Fc) as electron donors. Upon addition of Me_8Fc to a CH_3CN solution containing **1**, we observed the increase of absorbance at 490 nm due to $Ru^{III}(O)$ and that at 760 nm due to Me_8Fc^+ (Fig. 4). The ET reaction obeyed pseudo-first-order kinetics in the presence of excess Me_8Fc (Fig. 4c). The pseudo-first-order rate constant (k_{obs})

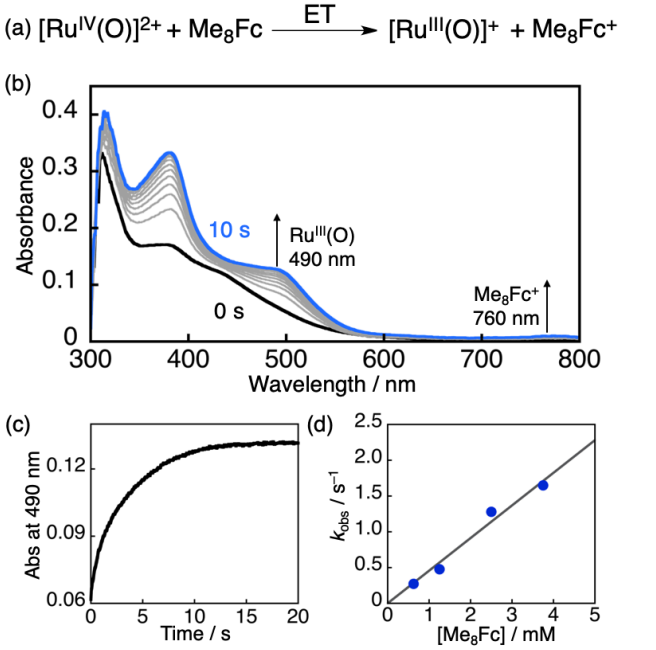

Fig. 4 (a) Reaction scheme for ET reduction of **1** by Me_8Fc. (b) UV-vis spectral change observed upon addition of Me_8Fc (1.25 mM) to a CH_3CN solution of **1** (25 μM) at 243 K. (c) The time profile of the absorbance at λ = 490 nm. (d) A plot of k_{obs} *vs.* [Me_8Fc] in the reaction of **1** with Me_8Fc.

increased linearly with increasing concentrations of Me_8Fc (Fig. 4d). The second-order ET rate constant (k_{et}) was determined from the slope of linear correlation of k_{obs} *vs.* [Me_8Fc] to be 4.6 × 10^2 M^{-1} s^{-1}. Similarly, k_{et} values for other electron donors were determined (Figs. S8 and S9 in the ESI†) as summarized in Table 1.

Although no ET reaction to **1** was observed in the case of ferrocene (Fc; E_{ox} = 0.37 V *vs.* SCE)[15] as an electron donor, addition of trifluoroacetic acid (TFA) to a CH_3CN solution containing **1** and Fc allowed us to observe a PCET reaction by UV-vis spectroscopy (Fig. S10 in the ESI†). As the PCET product derived from **1**, the Ru^{II}-OH_2 complex (**3**) was only observed without any intermediates. In addition, the PCET reaction was confirmed to be a $2e^-$ pathway by spectroscopic titration using $Me_{10}Fc$ as an electron donor (Fig. S11 in the ESI†). Thus, we conclude that the reduction of a Ru^{III} intermediate is faster than that of **1** in the presence of TFA.

Electrochemical measurements of **1** and **2** in the presence of TFA (pK_a = 12.6 in CH_3CN)[20] were performed to determine the E_{red} values of **1** and **2** in PCET reactions. The E_{red} value of **1** in the presence of TFA ([TFA] = 2.5 mM) was determined to be 0.69 V in CH_3CN at 298 K with a large positive shift (ΔE_{red} = 0.68 V) in comparison with that of **1** without TFA (Fig. S12 in the ESI†). Under the same conditions, the E_{red} value of **2** was determined

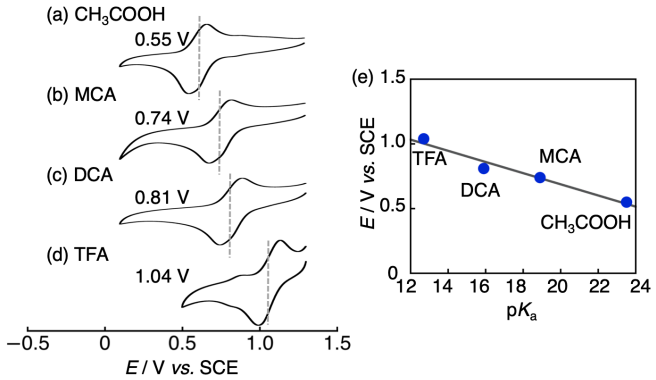

Fig. 5 CV traces for **1** (1.0 mM) in the presence of 550 mM acids: TFA (a), DCA (b), MCA (c), and CH_3COOH (d) in CH_3CN containing 0.1 M $TBAPF_6$ as an electrolyte at 298 K. (e) A plot of E values in the presence of acids (550 mM) relative to pK_a values of the acids used.

Table 1. E_{red} Values of Electron Donors and Second-Order Rate Constants (k_{et} and k_{pcet}) in ET or PCET by **1** or **2** at 243 K in CH_3CN.

Electron Donor	E_{ox} / V *vs.* SCE	$-\Delta G_{et}$ / eV		k_{et} / M^{-1} s^{-1}		$-\Delta G_{pcet}$ / eV		k_{pcet} / M^{-1} s^{-1}	
		1	**2**	**1**	**2**	**1**	**2**	**1**	**2**
$Me_{10}Fc$	–0.08	0.09	0.22	4.3 × 10^3	2.1 × 10^5	0.77	0.84	too fast	too fast
Me_8Fc	–0.04	0.05	0.18	4.6 × 10^2	2.3 × 10^3	0.73	0.80	too fast	too fast
Me_5Fc	0.15	–0.14	–0.01	1.4	7.2	0.54	0.61	too fast	too fast
BrFc	0.54	–0.53	–0.40	n.d.[b]	n.d.[b]	0.15	0.22	3.3 × 10^5	1.4 × 10^6
Br_2Fc	0.72	–0.71	–0.58	n.d.[b]	n.d.[b]	–0.03	0.04	2.1 × 10^4	4.4 × 10^5
Ph_3N	0.83	–0.82	–0.69	n.d.[b]	n.d.[b]	–0.14	–0.07	3.3 × 10^3	2.0 × 10^4
$(MeO)_3Ph$[a]	0.93	–0.92	–0.79	n.d.[b]	n.d.[b]	–0.24	–0.17	2.7 × 10	n.d.[b]

[a] 1,2,4-trimethoxybenzene. [b] n.d. denotes not determined.

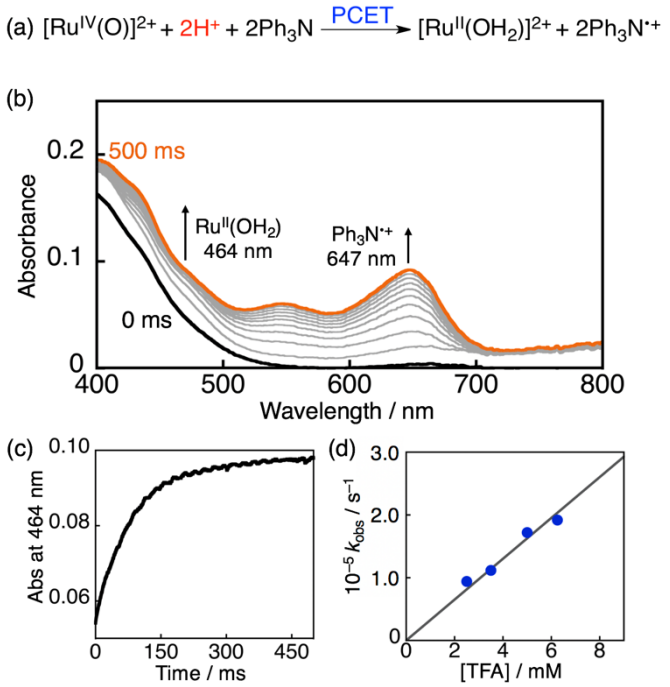

Fig. 6 (a) Reaction scheme for PCET reduction of **1** by Ph_3N in the presence of TFA. (b) UV-vis spectral change observed upon addition of Ph_3N (3.5 mM) to a CH_3CN solution containing **1** (25 μM) and TFA (2.5 mM) at 243 K. Inset: The time profile of the absorbance at λ = 464 nm. (c) A plot of k_{obs} *vs.* [Ph_3N].

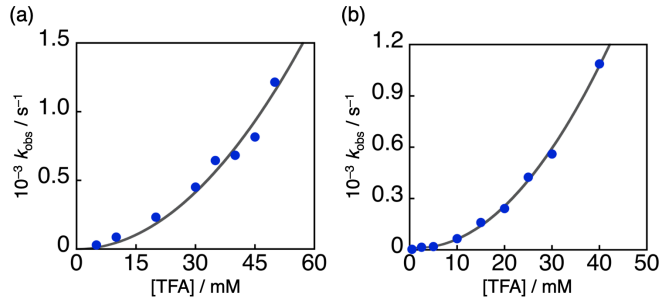

Fig. 7 A plot of k_{obs} *vs.* [TFA] in the PCET reaction from Ph_3N to (a) **1** (0.05 mM) or (b) **2** (0.03 mM) in the presence of Ph_3N (2.5 mM) in the presence of TFA in CH_3CN at 243 K.

to be 0.76 V, which was also positively shifted by 0.62 V from that without TFA. When TFA is replaced by weaker acids (550 mM) such as acetic acid (pK_a = 23.5),[20] monochloroacetic acid (MCA; pK_a = 18.9),[20] and dichloroacetic acid (DCA; pK_a = 15.9),[20] the E_{red} value of **1** is lower (0.55 V, 0.74 V, and 0.81 V, respectively) than that in the presence of 550 mM TFA (1.04 V) (Fig. 5). The E_{red} value depends on pK_a values with the slope (–43 mV/pK_a), indicating that PCET reactions correlate with the apparent proton concentration ([H^+]) in CH_3CN.[6b]

On the basis of the E_{red} values of **1** and **2** in the presence of TFA (2.5 mM), ET reactions from several electron donors to **1** and **2** were investigated in CH_3CN at 243 K in light of the Marcus theory of ET. Addition of triphenylamine (Ph_3N) as an electron donor, which was not protonated by TFA, to **1** in the presence of TFA resulted in the formation of **3** at 464 nm and $Ph_3N^{\bullet+}$ at 647 nm[21] as shown in Fig. 6. The second-order PCET rate constants (k_{pcet}) for electron donors were determined by the same procedures of k_{et} determination, which are summarized in Table 1 and Figs. S13 and S14 in the ESI†. The driving force ($-\Delta G_{pcet}$) of PCET was calculated based on the difference between E_{red} values in the presence of TFA (2.5 mM) and E_{ox} values of electron donors. It should be noted that the E_{ox} values of electron donors are not affected by the presence of TFA. When we investigated the [TFA] dependence of the k_{obs} value for PCET from Ph_3N to **1** and **2**, the k_{obs} values showed second-order dependence on [TFA] (Fig. 7). This result indicates that two protons are involved in the PCET from Ph_3N to $Ru^{IV}(O)$ species (Fig. 6a), whereas the amount of protonated $Ru^{IV}(O)$ species is negligible to be detected under the reaction conditions.[6c]

The driving-force dependence of k_{et} and k_{pcet} values was analyzed in light of the Marcus theory of adiabatic ET (eqn 2),

$$k = Z\exp[-(\lambda/4)(1 + \Delta G/\lambda)^2/k_BT] \quad (2)$$

where Z is the collision frequency (1×10^{11} M^{-1} s^{-1} in CH_3CN), λ is the reorganization energy of ET, k_B is the Boltzmann constant, and T is the absolute temperature.[22] The λ values of **1** and **2** in ET were determined to be 1.70 ± 0.06 eV and 1.88 ± 0.03 eV, respectively, in CH_3CN at 243 K on the basis of the Marcus plots in Fig. 8. It should be noted that the previously reported λ values of $Fe^{IV}(O)$, $Mn^{IV}(O)$, and $Cr^{V}(O)$ complexes in ET are summerized in Table 2. These λ values of $Ru^{IV}(O)$ complexes in ET (1.70–1.88 eV) were clearly smaller than those of $Fe^{IV}(O)$ complexes (2.00–2.74 eV)[5b,17] and $Mn^{IV}(O)$ complexes (2.24–2.27 eV)[6d] because of the lack of participation of d_σ orbitals in the ET reactions of $Ru^{IV}(O)$ complexes. In addition, the λ values of **1** and **2** in PCET were also determined to be 1.26 ± 0.04 eV and 1.20 ± 0.07 eV, which are much smaller than those of ET. In sharp contrast to the cases of **1** and **2**, negligible changes of λ values have been reported in the case of $Fe^{IV}(O)$ and $Mn^{IV}(O)$ complexes as shown in Table 2. The significant difference between λ values of $Ru^{IV}(O)$ complexes in ET and PCET is assumed to be derived from the difference of averaged structural changes before and after ET or PCET reactions.

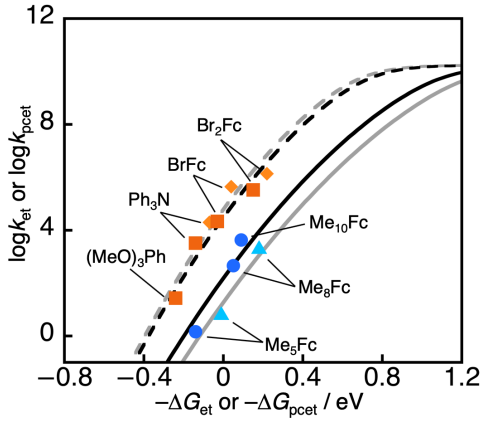

Fig. 8 Marcus plots of logk_{et} against driving forces of ET for ET reactions **1** (blue circle) and **2** (light blue triangle) in CH_3CN at 243 K, and those of logk_{pcet} for PCET reactions in the presence of TFA (2.5 mM) **1** (red square) and **2** (orange diamond) in CH_3CN at 243 K, respectively.

Table 2. Comparison of E_{red} values and λ values of $M^{n+}(O)$

$M^{n+}(O)$	E_{red}[a] / V	λ_{ET} / eV	λ_{PCET} / eV	ref
1	0.01	1.70 ± 0.06	1.26 ± 0.04	This work
2	0.14	1.88 ± 0.03	1.20 ± 0.07	This work
$Fe^{IV}(O)$(Bispidine)	0.37-0.73	2.00 – 2.28	n.d.[b]	5b
$Fe^{IV}(O)$(N4Py)	0.51	2.74 ± 0.06	2.74	6b, 17
$Fe^{IV}(O)$(TMC)	0.39	2.37 ± 0.04	n.d.[b]	17
$Mn^{IV}(O)$(N4Py)	0.80	2.27 ± 0.03	2.20 ± 0.02	6d,6e
$Mn^{IV}(O)$(BnTPEN)	0.78	2.24 ± 0.03	2.15 ± 0.03	6d,6e
$Cr^{V}(O)$(TPA-COO)	1.23	1.03 ± 0.05	n.d.	23

[a] E_{red} values (V / vs SCE) of $M^{n+}(O)$ without acids [b] n.d. denotes not determined.

Theoretical calculations

In order to gain deeper insights into the ET and PCET reactions of **1**, DFT calculations were performed to clarify the structural change between **1** and the $Ru^{III}(O)$ species in the absence and presence of two TFA molecules by comparing bond lengths around the Ru centres. In the absence of TFA, the averaged change of the coordination bond lengths around the Ru centre is determined to be 0.058 Å as shown in Fig. S15 in the ESI†. On the other hand, the Ru^{III}-O species is protonated to be a $Ru^{III}(OH)$ complex in the presence of TFA as demonstrated by DFT calculations (Fig. S16 in the ESI†). In this case, the hydrogen bonding of TFA with the oxo ligand elongates the Ru-O bond in **1** prior to the PCET reaction. The elongation should cause the smaller structural change in PCET than that in ET as represented by the difference of the averaged bond length change of 0.043 Å in PCET (Fig. S16 in the ESI†) than that (0.058 Å) in ET mentioned above. The order of magnitudes of the structural changes calculated for **1** in ET and PCET is consistent with that of the λ values of ET and PCET obtained by the kinetic analysis based on the Marcus theory of ET.

Conclusions

In summary, we have successfully determined the reorganization energies (λ) of ET and PCET of $Ru^{IV}(O)$ complexes in light of the Marcus theory of ET for the first time. The obtained smaller λ values of $Ru^{IV}(O)$ complexes than those of $Fe^{IV}(O)$ and $Mn^{IV}(O)$ complexes were interpreted by the smaller structural change for the $Ru^{IV}(O)$ complexes owing to the lack of participation of d_σ orbitals in the ET or PCET reactions. In addition, the λ value of PCET for **1** is much smaller than that of ET to indicate that the PCET process for **1** proceeds much more effectively than ET in terms of reaction rates. The determination of λ values for $Ru^{IV}(O)$ species reported here will contribute the further understanding the controlling factors in oxidation reactions by high-valent Ru-oxo complexes.

Experimental Section

General. UV-vis absorption spectra were measured in acetonitrile (CH_3CN) on Agilent 8453 and 8454 spectrometers at various temperatures with a cryostat (CoolSpek from UNISOKU) and a UNISOKU USP-SFM-CRD10 double mixing stopped-flow apparatus at 243 K under N_2. ^1H NMR spectra were recorded on a Bruker AVANCE400 spectrometer. CH_3CN was distilled over CaH_2 under Ar prior to use. Toluene was distilled from Na/benzophenone under Ar before use. Chemicals were used as received unless otherwise noted. Mebpa[24] and $[Ru^{III}Cl_3(Mebpa)]$[25] were synthesized according to literature methods.

$[Ru^{II}Cl(Mebpa)(bpy)](PF_6)$. $[Ru^{III}Cl_3(Mebpa)]$ (502.0 mg, 1.19 mmol) and LiCl (125.0 mg, 2.95 mmol) were added in an EtOH:water = 3:1 (v/v) mixed solvent (120 mL), and stirred for 10 min at 323 K. NEt_3 (0.4 mL, 0.287 mmol) was added to the reaction mixture. The mixture was stirred for 20 min to form a dark green solution. 2,2'-Bipyridine (247.5 mg, 1.56 mmol) was added to the reaction mixture and refluxed for 4 h to afford a dark red solution. The reaction mixture was concentrated to a small volume under reduced pressure. NH_4PF_6 (797.5 mg, 4.89 mmol) in water was added to the solution to afford the brown precipitate. The precipitate was collected by filtration and dried under vacuum to obtain a dark red powder. The red powder was recrystallized from 2-propanol, and the resulting precipitate was filtered and dried under vacuum to obtain the reddish brown powder of the title compound in 58% yield (447.6 mg, 0.69 mmol). ^1H NMR (acetone-d_6): δ2.13 (s, 3H, -CH_3), 4.38 (ABq, 4H, *J* = 16 Hz, -CH_2-), 7.42-7.53 (m, 6H, *bpy*-3H, *bpy*-5H and *Mebpa*-4H), 7.84 (t, 2H, *J* = 8.0 Hz, *Mebpa*-5H), 8.04 (t, 2H, *J* = 8.0 Hz, *bpy*-4H), 8.48 (d, 2H, *J* = 4.0 Hz, *Mebpa*-3H), 8.70 (d, 2H, *J* = 8.0 Hz, *bpy*-6H), 9.62 (d, 2H, *J* = 8.0 Hz, *Mebpa*-6H). Anal. Calcd for $C_{23}H_{23}ClF_6N_5PRu\bullet0.75H_2O\bullet0.4$acetone: C, 42.27; H, 3.94; N, 10.18. Found: C, 42.01; H, 3.63; N, 9.88. The amount of acetone was confirmed by ^1H NMR measurements in CD_3OD.

$[Ru^{II}(Mebpa)(bpy)(OH_2)](PF_6)_2$ ($3\bullet(PF_6)_2$). A solution of $[Ru^{II}Cl(Mebpa)(bpy)](PF_6)$ (127.8 mg, 0.196 mmol) in water (80 mL) was stirred for 1 h at 323 K. $AgNO_3$ (37.3 mg, 0.220 mmol) in water was added to the mixture and the mixture was heated at 333 K for 5 h. The reaction mixture was filtered through a filter paper to remove AgCl. The filtrate was concentrated to a small volume under reduced pressure. NH_4PF_6 (307.7 mg, 1.89 mmol) in water was added to the concentrated filtrate and the solution was cooled in a refrigerator to form a red precipitate. The red precipitate was collected by filtration, washed with water and dried under vacuum to obtain a red powder of the title compound in 72% yield (110.4 mg, 0.142 mmol). ^1H NMR (D_2O): δ1.92 (s, 3H, -CH_3), 4.16 (s, 4H, -CH_2-), 7.37-7.49 (m, 6H, *bpy*-3H, *bpy*-5H and *Mebpa*-4H), 7.79 (t, 2H, *J* = 8.0 Hz, *Mebpa*-5H), 8.05 (t, 2H, *J* = 8.0 Hz, *bpy*-4H), 8.50 (d, 2H, *J* = 8.0 Hz, *Mebpa*-3H), 8.57 (d, 2H, *J* = 8.0 Hz, *bpy*-6H), 8.82 (d, 2H, *J* = 8.0 Hz, *Mebpa*-6H). Anal. Calcd for $C_{23}H_{25}F_{12}N_5OP_2Ru$: C, 35.49; H, 3.24; N, 9.00. Found: C, 35.43; H, 3.01; N, 8.89.

$[Ru^{IV}(O)(Mebpa)(bpy)](PF_6)_2$ ($1\cdot(PF_6)_2$). $[Ru^{II}(Mebpa)(bpy)(OH_2)](PF_6)_2$ (10.56 mg, 0.014 mmol) was dissolved in water (5 mL). The solution was stirred for 50 min and $(NH_4)_2[Ce^{IV}(NO_3)_6]$ (CAN) (15.88 mg, 0.029 mmol) was added as an oxidant to the solution. Color of the solution changed from red to yellow. KPF_6 (5.67 mg, 0.031 mmol) dissolved in water was added to the reaction mixture and the solution was cooled in a refrigerator to form a light green crystal. The crystal was collected by filtration, dried under vacuum to obtain a light green crystal in 29% yield (3.17 mg, 0.004 mmol).

^{1}H NMR (CD_3CN): δ –19.2, 11.7, 12.9, 17.4, 56.5. Anal. Calcd for $C_{23}H_{23}F_{12}N_5OP_2Ru$: C, 35.58; H, 2.99; N, 9.02. Found: C, 35.31; H, 2.86; N, 9.22.

$[Ru^{IV}(O)(bpy)_2(py)](ClO_4)_2$. ($2\cdot(ClO_4)_2$). $[Ru^{II}(bpy)_2(py)(OH_2)](ClO_4)_2$ (2.43 mg, 0.003 mmol) was dissolved in water (2 mL). The solution was stirred for 20 min, and $Ce^{IV}(SO_4)_2\bullet H_2O$ (6.81 mg, 0.017 mmol) was added as an oxidant to the solution. The solution was stirred for 20 min and filtered through a membrane filter to remove insoluble solids. When the filtrate with 1 drop of sat. $NaClO_4$ was cooled at refrigerator for 3 days, a green crystal was appeared. The crystal was filtered and dried under vacuum to obtain green crystals in 52% yield (1.10 mg, 0.2 μmol). ^{1}H NMR (CD_3CN): δ –41.3, –31.4, –28.1, –23.1, –19.2, –10.9, –8.6, 6.6, 12.6, 12.8, 13.0, 13.7, 14.7, 18.2, 26.2, 51.0, 53.7. Anal. Calcd for $C_{25}H_{21}Cl_2N_5O_9Ru\bullet 0.5H_2O$: C, 41.91; H, 3.10; N, 9.78. Found: C, 42.03; H, 2.96; N, 9.74.

Me_5Fc (1,2,3,4,5-pentamethylferrocene). Cyclopentadienyliron(I) dicarbonyl dimer (533 mg, 1.51 mmol) was dissolved in distilled toluene (20 mL) and 1,2,3,4,5-pentamethylcyclopentadiene (1.6 mL, 9.86 mmol) was added to the solution. After three freeze-pump thaw (FPT) cycles, the solution was stirred for 69 h at 353-363 K. The reaction mixture was filtered through a filter paper to eliminate remaining Fe^I precipitate. The filtrate was concentrated to a small volume under vacuum, and the residue was dissolved in small volume of hexane. The hexane solution was purified by silica gel chromatography eluted with hexane including 0.5% NEt_3. The yellow fraction was collected and the solvent was evaporated under vacuum. The residual solid was recrystallized from acetone and H_2O, and dried under vacuum to obtain yellow powder in 30% yield. ^{1}H NMR (acetone-d_6): δ1.90 (s, 15H, Cp^{*-}), 3.66 (s, 5H, Cp^-). Anal. Calcd for $C_{15}H_{20}Fe$: C 70.33, H 7.87; Found: C 70.38, H 7.74.

X-ray Crystallography. Red-colored single crystals of $[Ru^{II}(Mebpa)(bpy)(OH_2)](PF_6)_2$ were obtained by recrystallization from a mixed solvent (EtOH:water = 3:1 (v/v)) with diffusion of AcOEt. Light-green-colored single crystals of **$1\cdot(PF_6)_2$** were grown by cooling an aqueous solution of crude **$1\cdot(PF_6)_2$** in a refrigerator overnight. Green-colored single crystals of **$2\cdot(ClO_4)_2$** were grown by cooling an aqueous solution of **$2\cdot(ClO_4)_2$** with 1 drop of saturated $NaClO_4$ aqueous solution in a refrigerator for 3 days. A single crystal was mounted on a mounting loop. X-ray diffraction measurements on **$1\cdot(PF_6)_2$** and **$3\cdot(PF_6)_2$** were performed at 120 K on a Bruker APEXII Ultra diffractometer at University of Tsukuba. Those on **$2\cdot(ClO_4)_2$** were performed at 93 K on a Rigaku XtaLAB AFC12 diffractometer at Rigaku Corp., Akishima, Tokyo, Japan. The structures were solved by a direct method (SIR-97 and SHELXL-97)[26] and expanded with differential Fourier technique. All non-hydrogen atoms were refined anisotropically and the refinement was carried out with full matrix least squares on *F*. All calculations were performed using the Yadokari-XG crystallographic software package.[27] In the structure refinements, the exact positions of the solvent molecules of crystallization could not be determined because of their severe disorder. Their contribution was thus subtracted from the diffraction pattern by the "Squeeze" program.[28] Supplementary crystallographic data of **$3\cdot(PF_6)_2$**, **$2\cdot(ClO_4)_2$**, and **$1\cdot(PF_6)_2$** are available from the Cambridge Crystallographic Data Center as CCDC 1881732-1881734, respectively.

Resonance Raman Spectroscopy on 1. Samples were prepared by the modified procedures as described above for $[Ru^{IV}(^{16}O)(Mebpa)(bpy)]^{2+}$. $[Ru^{IV}(^{18}O)(Mebpa)(bpy)]^{2+}$ was prepared by changing $H_2{}^{16}O$ to $H_2{}^{18}O$ as an oxygen source. Resonance Raman spectra were measured in CD_3CN at 243 K under photoexcitation at 441.6 nm with a He-Cd laser (Kimmon Koha, IK5651R-G), dispersed by a single polychromator (Ritu Oyo Kougaku Co., Ltd., MC-100DG) and detected by a liquid-nitrogen-cooled CCD detector (HORIBA JOBIN YVON, Symphony CCD-1024 × 256-OPEN-1LS). Raman shifts were calibrated using indene and carbon tetrachloride, providing an accuracy of ±1 cm^{-1} for intense isolated lines. The measurements were performed at 243 K using a spinning NMR tube (outer diameter = 5 mm, wall thickness = 0.2 mm) at 135° scattering geometry.

Electrochemical Measurements. Cyclic voltammetry (CV) and square wave voltammetry (SWV) measurements were carried out in CH_3CN containing 0.1 M $TBAPF_6$ as an electrolyte at 298 K under Ar using a BAS ALS-710D electrochemical analyzer with a platinum working electrode, a platinum wire as a counter electrode, and $Ag/AgNO_3$ as a reference electrode. The potentials measured were calibrated to be those relative to SCE by adding 0.29 V.[29]

ESR Measurements. ESR spectra were recorded on a Bruker BioSpin X-band spectrometer (EMXPlus9.5/2.7) with an ESR900 helium-flow cryostat (Oxford Instruments) in a quartz tube (o.d. = 4 mm). The magnitude of the modulation was chosen to optimize the resolution and the signal to noise (S/N) ratio of the observed spectrum under non-saturating microwave power conditions (microwave power, 5.0 mW; modulation amplitude, 15.0 G; modulation frequency, 100 kHz). An ESR sample of Ru^{III} species was prepared by mixing **1** (1.0 mM) and 1.0 eq. of Me_8Fc as a reductant in CH_3CN at room temperature. After bubbling He into the prepared solution, the sample solution was transferred in quartz tubes under He atmosphere.

Computational Methods. All calculations were performed by the Gaussian 16 program package.[30] We optimized local minima on the potential energy using the B3LYP method.[31] For the Ru atom, we used the SDD basis sets,[32] and for the H, C, N, O, and F atoms, we used the D95** basis set.[33] Vibration frequencies were systematically computed in order to ensure that on a potential energy surface each optimized geometry corresponds to a local minimum that has no imaginary frequency. Solvent effect of acetonitrile was included using the corresponding polarizable continuum model (PCM).[34]

Conflicts of interest

There are no conflicts to declare.

Acknowledgements

This work was supported by Grants-in-Aid (Nos. 17H03027, and 17K14456) from the Japan Society of Promotion of Science (JSPS,

MEXT) of Japan and the Cooperative Research Program of "Network Joint Research Center for Materials and Devices". Financial supports through CREST (JST) are also appreciated (JPMJCR16P1 for T.K. and JPMJCR15P5 for K.Y.). We also appreciate Dr. Takashi Kikuchi (Rigaku Corporation) for cooperation in X-ray crystallographic analysis on **2**.

Notes and references

1 (*a*) L. Que, Jr. and R. Y. N. Ho, *Chem. Rev.,* 1996, **96**, 2607-2624; (*b*) C. Krebs, D.Galonic Fujimori, C. T. Walsh and J. M. Bollinger, *Acc. Chem. Res*., 2007, **40**, 484-492.

2 (*a*) W. Nam, *Acc. Chem. Res*., 2007, **40**, 522-531; (*b*) L. Que, Jr., *Acc. Chem. Res.,* 2007, **40**, 493-500; (*c*) D. Goldberg, *Acc. Chem. Res.,* 2007, **40**, 626-634.

3 (*a*) J. M. Mayer, *Acc. Chem. Res.,* 2011, **44***,* 36-46; (*b*) W. Nam, Y.-M. Lee, S. Fukuzumi, *Acc. Chem. Res.,* 2014, **47**, 1146-1154.

4 (*a*) J. M. Mayer, *Annu. Rev. Phys. Chem*., 2004, **55**, 363-390; (*b*) J. J. Warren, T. A. Tronic and J. M. Mayer, *Chem. Rev*., 2010, **110**, 6961-7001; (*c*) D. R. Weinberg, C. J. Gagliardi, J. F. Hull, C. F. Murphy, C. A. Kent, B. C. Westlake, A. Paul, D. H. Ess, D. G. McCafferty and T. J. Meyer, *Chem. Rev.,* 2012, **112**, 4016-4093.

5 (*a*) W. Fenwick, A. M. English and J. F. Wishart, *J. Am. Chem. Soc.,* 1997, **119**, 4758-4764; (*b*) P. Comba, S. Fukuzumi, C. Koke, B. Martin, A.-M. Löhr and J. Straub, *Angew. Chem., Int. Ed.*, 2016, **55**, 11129-11133; (*c*) H. Bataineh, O. Pestovsky and A. Bakac, *Inorg. Chem.*, 2016, **55**, 6719-6724.

6 (*a*) S. Fukuzumi, *Coord. Chem. Rev.,* 2013, **257**, 1564-1575; (*b*) J. Park, Y. Morimoto, Y.-M. Lee, W. Nam and S. Fukuzumi, *J. Am. Chem. Soc.,* 2012, **134**, 3903-3911; (*c*) J. Park, Y.-M. Lee, W. Nam and S. Fukuzumi, *J. Am. Chem. Soc.,* 2013, **135**, 5052-5061; (*d*) H. Yoon, Y.-M. Lee, X. Wu, K.-B. Cho, R. Sarangi, W. Nam and S. Fukuzumi, *J. Am. Chem. Soc.,* 2013, **135**, 9186-9194; (*e*) J. Chen, H. Yoon, Y.-M. Lee, M. S. Seo, R. Sarangi, S. Fukuzumi and W. Nam, *Chem. Sci.*, 2015, **6**, 3624-3632.

7 (*a*) J. R. Bryant and J. M. Mayer, *J. Am. Chem. Soc.,* 2003, **125**, 10351-10361; (*b*) C. R. Waidmann, X. Zhou, E. A. Tsai, W. Kaminsky, D. A. Hrovat, W. T. Borden and J. M. Mayer, *J. Am. Chem. Soc.,* 2009, **131**, 4729-4743.

8 (*a*) J. M. Mayer, *Acc. Chem. Res.,* 1998, **31**, 441-450; (*b*) H. Mitome, T. Ishizuka, H. Kotani, Y. Shiota, K. Yoshizawa and T. Kojima, *J. Am. Chem. Soc.*, 2016, **138**, 9508-9520.

9 C.-M. Che, V. W.-W. Yam and T. C. W. Mak, *J. Am. Chem. Soc.,* 1990, **112**, 2284-2291.

10 (*a*) B. A. Moyer, M. S. Thompson and T. J. Meyer, *J. Am. Chem. Soc.,* 1980, **102**, 2310-2312; (*b*) B. A. Moyer and T. J. Meyer, *Inorg. Chem.,* 1981, **20**, 436-444; (*c*) J. Gilbert, L. Roecker and T. J. Meyer, *Inorg. Chem.,* 1987, **26**, 1126-1132; (*d*) J. J. Concepcion, J. W. Jurss, J. L. Templeton and T. J. Meyer, *Proc. Natl. Acad. Sci. U.S.A.,* 2008, **105**, 17632-17635.

11 (*a*) J. T. Groves and R. Quinn, *Inorg. Chem.,* 1984, **23**, 3844-3846; (*b*) J. T. Groves and R. Quinn, *J. Am. Chem. Soc.,* 1985, **107**, 5790-5792.

12 (*a*) Y. Hirai, T. Kojima, Y. Mizutani, Y. Shiota, K. Yoshizawa and S. Fukuzumi, *Angew. Chem., Int. Ed.,* 2008, **47**, 5772-5776; (*b*) T. Kojima, K. Nakayama, K. Ikemura, T. Ogura and S. Fukuzumi, *J. Am. Chem. Soc.,* 2011, **133**, 11692-11700; (*c*) T. Ishizuka, H. Kotani and T. Kojima, *Dalton Trans.,* 2016, **45**, 16727-16750.

13 M. Rodríguez, I. Romero, A. Llobet, A. Deronzier, M. Biner, T. Parella and H. Stoeckli-Evans, *Inorg. Chem.,* 2001, **40**, 4150-4156.

14 Detailed characterization of the Ru^{III} species is underway with various techniques, such as resonance Raman spectroscopy and electrospray mass spectrometry.

15 T. Gennett, D. F. Milner and M. J. Weaver *J. Phys. Chem.,* 1985, **89**, 2787-2794.

16 N. Gauthier, N. Tchouar, F. Justaud, G. Argouarch, M. P. Cifuentes, L. Toupet, D. Touchard, J.-F. Halet, S. Rigaut, M. G. Humphrey, K. Costuas and F. Paul, *Organometallics*, 2009, **28**, 2253-2266.

17 Y.-M. Lee, H. Kotani, T. Suenobu, W. Nam and S. Fukuzumi, *J. Am. Chem. Soc.,* 2008, **130***,* 434-435.

18 Complex **1** was regenerated from the reduced Ru(III) complex with use of tris(4-bromophenyl)ammoniumyl hexachloroantimonate as a one-electron oxidant to confirm the ET equilibrium (Fig. S7 in the ESI†).

19 (*a*) T. Kojima, R. Kobayashi, T. Ishizuka, S. Yamakawa, H. Kotani, T. Nakanishi, K. Ohkubo, Y. Shiota, K. Yoshizawa and S. Fukuzumi, *Chem.–Eur. J.,* 2014, **20**, 15518-15532; (*b*) W. Suzuki, H. Kotani, T. Ishizuka, K. Ohkubo, Y. Shiota, K. Yoshizawa, S. Fukuzumi and T. Kojima, *Chem.–Eur. J.,* 2017, **23**, 4669-4679.

20 K. Izutsu, in *Acid–Base Dissociation Constants in Dipolar Aprotic Solvents*, Blackwell Scientific Publications, Oxford, 1990.

21 A. Saeki, S. Seki, N. Satoh, K. Yamamoto and S. Tagawa, *J. Phys. Chem. B,* 2008, **112**, 15540-15545.

22 (*a*) R. A. Marcus, *Annu. Rev. Phys. Chem*., 1964, **15**, 155-196; (*b*) R. A. Marcus, *Angew. Chem., Int. Ed. Engl*., 1993, **32**, 1111-1121.

23 H. Kotani, S. Kaida, T. Ishizuka, M. Sakaguchi, T. Ogura, Y. Shiota, K. Yoshizawa and T. Kojima, *Chem. Sci.,* 2015, **6**, 945-955.

24 K. B. Jensen, C. J. McKenzie, O. Simonsen, H. Toftlund, A. Hazell, *Inorganic Chim. Acta,* 1997, **257**, 163.

25 Y. Shimizu, S. Fukui, T. Oi and H. Nagao, *Bull. Chem. Soc. Jpn.,* 2008, **81**, 1285.

26 G. M. Sheldrick, SIR97 and SHELXL-97, Program for Crystal Structure Refinement, University of Göttingen, Göttingen (Germany), 1997.

27 C. Kabuto, S. Akine, T. Nemoto and E. Kwon, Release of Software (Yadokari-XG 2009) for Crystal Structure Analyses, *J. Cryst. Soc. Jpn.,* 2009, **51**, 218-224.

28 P. V. D. Sluis and A. L. Spek, *Acta Crystallogr.,* 1990, **A46**, 194-201.

29 T. Nakanishi, K. Ohkubo, T. Kojima and S. Fukuzumi, *J. Am. Chem. Soc.,* 2009, **131**, 577-584.

30 Gaussian 16, Revision A.03, M. J. Frisch, G. W. Trucks, H. B. Schlegel, G. E. Scuseria, M. A. Robb, J. R. Cheeseman, G. Scalmani, V. Barone, G. A. Petersson, H. Nakatsuji, X. Li, M. Caricato, A. V. Marenich, J. Bloino, B. G. Janesko, R. Gomperts, B. Mennucci, H. P. Hratchian, J. V. Ortiz, A. F. Izmaylov, J. L. Sonnenberg, D. Williams-Young, F. Ding, F. Lipparini, F. Egidi, J. Goings, B. Peng, A. Petrone, T. Henderson, D. Ranasinghe, V. G. Zakrzewski, J. Gao, N. Rega, G. Zheng, W. Liang, M. Hada, M. Ehara, K. Toyota, R. Fukuda, J. Hasegawa, M. Ishida, T. Nakajima, Y. Honda, O. Kitao, H. Nakai, T. Vreven, K. Throssell, J. A. Montgomery, Jr., J. E. Peralta, F. Ogliaro, M. J. Bearpark, J. J. Heyd, E. N. Brothers, K. N. Kudin, V. N. Staroverov, T. A. Keith, R. Kobayashi, J. Normand, K. Raghavachari, A. P. Rendell, J. C. Burant, S. S. Iyengar, J. Tomasi, M. Cossi, J. M. Millam, M. Klene, C. Adamo, R. Cammi, J. W. Ochterski, R. L. Martin, K. Morokuma, O. Farkas, J. B. Foresman and D. J. Fox, Gaussian, Inc., Wallingford CT, 2016.

31 A. D. Becke, *J. Chem. Phys.,* 1993, **98**, 5648–5652.

32 D. Andrae, U. Häußermann, M. Dolg, H. Stoll and H. Preuß, *Theor. Chem. Acc.,* 1990, **77**, 123-141.

33 T. H. Dunning and P. J. Hay, In *Modern Theoretical Chemistry*; H. F. Schaefer, III, Ed.; Plenum: New York, 1976; Vol. 3, pp 1-27.

34 J. Tomasi, B. Mennucci and R. Cammi, *Chem. Rev.,* 2005, **105***,* 2999-3094.

TOC graphic

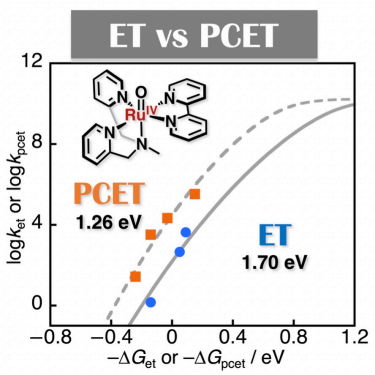

Reorganization energies (λ) in electron transfer (ET) and proton-coupled ET (PCET) from electron donors to isolated $Ru^{IV}(O)$ complexes were determined to be in the range of 1.70–1.88 eV (ET) and 1.20–1.26 eV (PCET).